

# Simple inflationary models in Gauss-Bonnet brane-world cosmology

Nobuchika Okada <sup>a</sup> and Satomi Okada

<sup>a</sup>*Department of Physics and Astronomy, University of Alabama, Tuscaloosa, AL35487, USA*

## Abstract

In light of the recent measurements of the CMB anisotropy by the WMAP and Planck satellite experiments and the observation of CMB  $B$ -mode polarization announced by the BICEP2 collaboration, we study simple inflationary models in the context of the Gauss-Bonnet brane-world cosmology. The brane-world cosmological effect modifies the power spectra of scalar and tensor perturbations generated by inflation and causes a dramatic change for the inflationary predictions of the spectral index ( $n_s$ ) and the tensor-to-scalar ratio ( $r$ ) from those obtained in the standard cosmology. In particular, the power spectrum of tensor perturbation is suppressed due to the Gauss-Bonnet brane-world cosmological effect, which is in sharp contrast with inflationary scenario in the Randall-Sundrum brane-world cosmology where the power spectrum is enhanced. Hence, these two brane-world cosmological scenarios are distinguishable. With the dramatic change of the inflationary predictions, the inflationary scenario in the Gauss-Bonnet brane-world cosmology can be tested by more precise measurements of  $n_s$  and future observations of the CMB  $B$ -mode polarization.



# 1 Introduction

Inflationary universe is the standard paradigm in the modern cosmology [1, 2, 3, 4], by which serious problems of the standard big-bang cosmology, such as the flatness and horizon problems, can be solved. In addition, inflationary universe provides the primordial density fluctuations as seeds for the formation of the large scale structure observed in the present universe. Various inflation models have been proposed with typical inflationary predictions for the spectral index ( $n_s$ ), the tensor-to-scalar ratio ( $r$ ), the running of the spectral index ( $\alpha = dn_s/d\ln k$ ), and non-Gaussianity of the primordial perturbations. These predictions are currently tested by precise measurements of the cosmic microwave background (CMB) anisotropy by the Wilkinson Microwave Anisotropy Probe (WMAP) [5] and the Planck satellite [6] experiments. Future cosmological observations are expected to be more precise towards discriminating inflationary models.

Recently the Background Imaging of Cosmic Extragalactic Polarization (BICEP2) collaboration has reported the observation of CMB  $B$ -mode polarization [7], which has been interpreted as  $r = 0.20^{+0.07}_{-0.05}$  (68% confidence level). If confirmed, the BICEP2 result is the direct evidence of the cosmological inflation in the early universe and provides us with great progress in understanding inflationary universe. However, this result has a tension when we simply compare it with the upper bound on  $r < 0.11$  set by the Planck measurement [6] (see, however, [8]), and it has been pointed out that uncertainty of dust polarization can dominate the excess observed by the BICEP2 experiment [9]. Future observations of the  $B$ -mode polarization with different frequencies are crucial to confirm the BICEP2 result.

Motivated by the recent results by the WMAP and Planck experiments as well as the BICEP2, we study inflationary scenario in the context of the brane-world cosmology. The brane-world cosmology is based on the so-called RS II model first proposed by Randall and Sundrum (RS) [10], where the Standard Model particles are confined on a "3-brane" at a boundary embedded in 5-dimensional anti-de Sitter (AdS) space-time. Because of the AdS space-time geometry, massless graviton in 4-dimensional effective theory is localized around the brane on which the Standard Model particles reside, while Kaluza-Klein gravitons are delocalized toward infinity. As a result, the 4-dimensional Einstein-Hilbert action is reproduced at low energies. A realistic cosmological solution in the RS II setup has been found in [11], which leads to the Friedmann equation in the 4-dimensional standard cosmology at low energies, while a non-standard expansion law at high energies. Since then, the RS II cosmology has been intensively studied [12]. The non-standard evolution of the early universe causes modifications of a variety of phenomena in particle cosmology, such as the dark matter relic abundance [13], baryogenesis via leptogenesis [14], and gravitino productions in the early universe [15]. A chaotic inflation



with a quadratic inflaton potential has been examined in [16], and it has been shown that the inflationary predictions are modified from those in the 4-dimensional standard cosmology. In particular, the power spectrum of tensor perturbation is found to be enhanced in the presence of the 5-dimensional bulk [17]. Taking the brane-world cosmological effects into account, the textbook chaotic inflation models with the quadratic and quartic potentials have been analyzed in [18]. Recently, in light of the BICEP2 result, the Higgs potential and the Coleman-Weinberg potential models, in addition to the textbook chaotic inflation models, have been analyzed [19]. It has been shown that these simple inflationary models except the quartic potential model can nicely fit the BICEP2 result with the enhancement of the tensor-to-scalar ratio due to the brane-world cosmological effects.

In this paper, we investigate the simple inflationary models in a more general brane-world cosmology, the Gauss-Bonnet (GB) brane-world cosmology, where the RS II model is extended by adding the Gauss-Bonnet invariant [20]. The Friedmann equation for the GB brane-world cosmology has been found in [21]), with which we analyze the inflationary models and compare the inflationary predictions with the recent cosmological observations. At high energies, where the GB invariant dominates the evolution of the universe (GB regime), the expansion law is quite different from that in the RS II cosmology.<sup>1</sup> Furthermore, it has been found that in the GB regime, the power spectrum of tensor perturbation is suppressed compared to that in the 4-dimensional standard cosmology [23]. Therefore, the inflationary predictions in the GB brane-world cosmology are altered from those in the standard cosmology as well as the RS brane-world cosmology.

In the next section, we briefly review the GB cosmological model and give the Friedmann equation in the GB regime. In Sec. 3, we analyze simple inflationary models based on the textbook models, the Higgs potential and the Coleman-Weinberg models. We obtain the inflationary predictions as a function of a parameter ( $\mu$ ) characterizing the GB brane-world cosmological effect and compare the predictions with the current observations. We also show responses of the parameters in the inflationary models, such as the inflaton mass, the inflaton self-coupling, and the inflaton vacuum expectation value (VEV), to the parameter  $\mu$ . The last section is devoted to conclusions.

## 2 The GB brane-world cosmology

Motivated by string theory considerations, it would be natural to extend the RS II cosmological model by adding higher curvature terms [20]. Among a variety of such terms, the GB invariant

---

<sup>1</sup> See [22] for the modification of dark matter physics in the GB brane-world cosmology.



is of particular interests in five dimensions, since it is a unique nonlinear term in curvature which yields second order gravitational field equations. The extended RS II action with the GB invariant is given by

$$\begin{aligned} \mathcal{S} = & \frac{1}{2\kappa_5^2} \int d^5x \sqrt{-g_5} [-2\Lambda_5 + \mathcal{R} + \alpha (\mathcal{R}^2 - 4\mathcal{R}_{ab}\mathcal{R}^{ab} + \mathcal{R}_{abcd}\mathcal{R}^{abcd})] \\ & - \int_{brane} d^4x \sqrt{-g_4} (m_\sigma^4 + \mathcal{L}_{matter}), \end{aligned} \quad (1)$$

where  $\kappa_5^2 = 8\pi/M_5^3$  with the five-dimensional Planck mass  $M_5$ ,  $m_\sigma^4 > 0$  is a brane tension, and  $\Lambda_5 < 0$  is the bulk cosmological constant. The limit  $\alpha \rightarrow 0$  recovers the RS II model.

Imposing a  $Z_2$  parity across the brane in an anti-de Sitter bulk and modeling the matters on the brane as a perfect fluid, the Friedmann equation on the spatially flat brane has been found to be [21]

$$\kappa_5^2(\rho + m_\sigma^4) = 2\mu \sqrt{1 + \frac{H^2}{\mu^2}} \left( 3 - \beta + 2\beta \frac{H^2}{\mu^2} \right), \quad (2)$$

where  $\beta = 4\alpha\mu^2 = 1 - \sqrt{1 + 4\alpha\Lambda_5/3}$ . The model has four free parameters,  $\kappa_5$ ,  $m_\sigma$ ,  $\mu$  and  $\beta$  (corresponding to the original parameters,  $\kappa_5$ ,  $\sigma$ ,  $\Lambda_5$  and  $\alpha$ ), which are constrained by phenomenological requirements as follows. To reproduce the Friedmann equation of the standard cosmology with a vanishing cosmological constant for the limit  $H^2/\mu^2 \ll 1$ , we have two conditions,

$$\kappa_5^2 m_\sigma^4 = 2\mu(3 - \beta), \quad \kappa_4^2 = 1/M_P^2 = \frac{\mu}{1 + \beta} \kappa_5^2, \quad (3)$$

where  $M_P = M_{Pl}/\sqrt{8\pi}$  is the reduced Planck mass with  $M_{Pl} = 1.22 \times 10^{19}$  GeV. From now on, we use the Planck unit,  $M_P = 1$ . The modified Friedmann equation can be rewritten in the useful form [24]

$$\begin{aligned} H^2 &= \frac{\mu^2}{\beta} \left[ (1 - \beta) \cosh \left( \frac{2\chi}{3} \right) - 1 \right], \\ \rho + m_\sigma^4 &= m_\alpha^4 \sinh \chi, \end{aligned} \quad (4)$$

where  $\chi$  is a dimensionless measure of the energy density and

$$m_\alpha^4 = \sqrt{\frac{8\mu^2(1 - \beta)^3}{\beta\kappa_5^4}} = 2\mu^2 \sqrt{2 \frac{(1 - \beta)^3}{\beta(1 + \beta)^2}}. \quad (5)$$

Here we have used Eq. (3) to eliminate  $\kappa_5$  in the last equality. In the same way, we express  $m_\sigma$  as

$$m_\sigma^4 = 2\mu^2 \left( \frac{3 - \beta}{1 + \beta} \right). \quad (6)$$



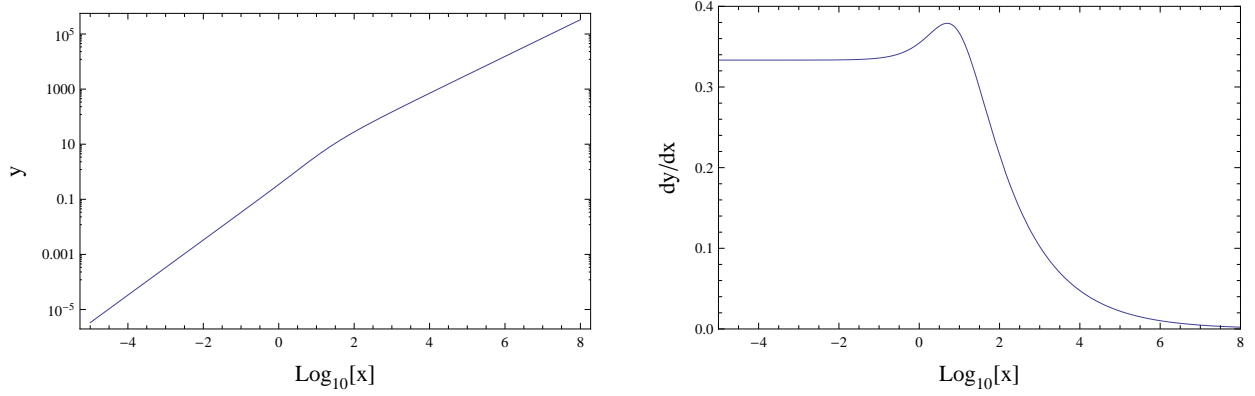


Figure 1: In the Planck unit ( $M_P = 1$ ),  $y = H^2/\mu^2$  as a function of  $x = \rho/\mu^2$  (left), and the first derivative of  $y$  with respect to  $x$  (right).

The evolution of the GB braneworld cosmology is characterized by the two mass scales,  $m_\alpha$  and  $m_\sigma$ . Expanding Eq. (4) with respect to  $\chi$ , we find three regimes for  $m_\alpha > m_\sigma$ . The GB regime for  $\rho \gg m_\alpha^4$ ,

$$H^2 \simeq \left( \frac{1+\beta}{4\beta} \mu \rho \right)^{2/3}, \quad (7)$$

the RS regime for  $m_\alpha^4 \gg \rho \gg m_\sigma^4$ ,

$$H^2 \simeq \frac{\rho^2}{6m_\sigma^4}, \quad (8)$$

and the standard regime for  $m_\sigma^4 \gg \rho$ ,

$$H^2 \simeq \frac{\rho}{3}. \quad (9)$$

Since we are interested in the GB regime, let us simplify the evolution of the universe by imposing the condition  $m_\alpha = m_\sigma$ , which leads to

$$3\beta^3 - 12\beta^2 + 15\beta - 2 = 0 \quad (10)$$

and hence,  $\beta = 0.151$ . In this case, the RS regime is collapsed, and there are only two regimes in the evolution of the universe. Now we rewrite the modified Friedmann equation as

$$(1+\beta) \frac{\rho}{\mu^2} + 2(3-\beta) = 2\sqrt{1 + \frac{H^2}{\mu^2}} \left( 3 - \beta + 2\beta \frac{H^2}{\mu^2} \right), \quad (11)$$

which is characterized by only one free parameter  $\mu$ . Solving this equation, we obtain  $H^2/\mu^2$  as a function of  $\rho/\mu^2$ . In Fig. 1, we plot  $y = H^2/\mu^2$  as a function of  $x = \rho/\mu^2$  (left) and the first derivative of  $y$  with respect to  $x$  (right). We can see that  $y \propto x^{2/3}$  for  $x \gg 1$  (GB regime), while  $y \propto x$  for  $x \ll 1$  (standard regime).



### 3 Simple inflationary models in GB brane-world cosmology

We first give basic formulas used in the following analysis for inflationary models. In the slow-roll inflation, the Hubble parameter is give by the solution of Eq. (11) with  $\rho = V(\phi)$ , where  $V$  is a potential of the inflaton field  $\phi$ . Since the inflaton is confined on the brane, the power spectrum of scalar perturbation obeys the same formula as in the standard cosmology, except for the modification of the Hubble parameter [16],

$$\mathcal{P}_S = \frac{9}{4\pi^2} \frac{H^6}{(V')^2}, \quad (12)$$

where the prime denotes the derivative with respect to the inflaton field  $\phi$ . For the pivot scale chosen at  $k_0 = 0.05 \text{ Mpc}^{-1}$ , the power spectrum of scalar perturbation is constrained as  $\mathcal{P}_S(k_0) = 2.215 \times 10^{-9}$  by the Planck satellite experiment [6]. By using the slow-roll parameters defined as

$$\epsilon = \frac{V'}{6H^2} (\ln H^2)', \quad \eta = \frac{V''}{3H^2}, \quad (13)$$

the spectral index is given by

$$n_s - 1 = \frac{d \ln \mathcal{P}_S}{d \ln k} = -6\epsilon + 2\eta. \quad (14)$$

Hence, the running of the spectral index,  $\alpha \equiv dn_s/d \ln k$ , is given by

$$\alpha = \frac{dn_s}{d \ln k} = \frac{V'}{3H^2} (6\epsilon' - 2\eta'). \quad (15)$$

On the other hand, in the presence of the extra dimension where graviton resides, the power spectrum of tensor perturbation is modified to be [23]

$$\mathcal{P}_T = 8 \left( \frac{H}{2\pi} \right)^2 F(x_0)^2, \quad (16)$$

where  $x_0 = \sqrt{H^2/\mu^2}$ , and

$$F(x) = \left( \sqrt{1+x^2} - \left( \frac{1-\beta}{1+\beta} \right) x^2 \ln \left[ \frac{1}{x} + \sqrt{1 + \frac{1}{x^2}} \right] \right)^{-1/2}. \quad (17)$$

For  $x \ll 1$ ,  $F(x)^2 \simeq 1$ , and Eq. (16) reduces to the formula in the standard cosmology. For  $x_0 \gg 1$ ,  $F(x)^2 \simeq \frac{1+\beta}{2\beta x} \simeq 3.81/x$ , so that the power spectrum of tensor perturbation is suppressed in the GB regime. Note that in the limit  $\beta = 0$ , the above  $F(x)$  is reduced to the one found for



the RS brane-world cosmology in [17]. In the RS case ( $\beta = 0$ ),  $F(x)^2 \simeq 1.5x$  for  $x \gg 1$ , and the power spectrum of tensor perturbation is enhanced. The tensor-to-scalar ratio is defined as  $r = \mathcal{P}_T/\mathcal{P}_S$ .

The e-folding number is given by

$$N_0 = \int_{\phi_e}^{\phi_0} d\phi \frac{3H^2}{V'}, \quad (18)$$

where  $\phi_0$  is the inflaton VEV at horizon exit of the scale corresponding to  $k_0$ , and  $\phi_e$  is the inflaton VEV at the end of inflation, which is defined by  $\max[\epsilon(\phi_e), |\eta(\phi_e)|] = 1$ . In the standard cosmology, we usually consider  $N_0 = 50 - 60$  in order to solve the horizon problem. Since the expansion rate in the GB brane-world cosmology is smaller than the standard cosmology case, we may expect a smaller value of the e-folding number. However, since the e-folding number also depends on reheating temperature after inflation, we consider  $N_0 = 50$  and  $60$  as reference values, as usual in the standard cosmology.

### 3.1 Textbook inflationary models

Let us first consider the textbook chaotic inflation model with a quadratic potential [3],

$$V = \frac{1}{2}m^2\phi^2. \quad (19)$$

In the standard cosmology, simple calculations lead to the following inflationary predictions:

$$n_s = 1 - \frac{4}{2N_0 + 1}, \quad r = \frac{16}{2N_0 + 1}, \quad \alpha = -\frac{8}{(2N_0 + 1)^2}. \quad (20)$$

The inflaton mass is determined so as to satisfy the power spectrum measured by the Planck satellite experiment,  $\mathcal{P}_S(k_0) = 2.215 \times 10^{-9}$ :

$$m[\text{GeV}] = 1.46 \times 10^{13} \left( \frac{60.5}{N_0 + 1/2} \right). \quad (21)$$

In the GB brane-world cosmology, these inflationary predictions in the standard cosmology are altered due to the modified Friedmann equation in Eq. (11). In the limit of  $H/\mu \gg 1$ , the Hubble parameter is simplified as

$$H^2 \simeq \left( \frac{1 + \beta}{4\beta} \mu V(\phi) \right)^{2/3}. \quad (22)$$

Using this expression, we can easily find the inflationary predictions of the form as

$$n_s = 1 - \frac{6}{4N_0 + 3}, \quad r = \frac{32}{4N_0 + 3}, \quad \alpha = -\frac{24}{(4N_0 + 3)^2}. \quad (23)$$



From the experimental constraint  $\mathcal{P}_S(k_0) = 2.215 \times 10^{-9}$ , we also find (in the Planck unit)

$$m\mu \simeq 3.44 \times 10^{-8} \left( \frac{4}{4N_0 + 3} \right)^{3/2} \quad (24)$$

Since  $\mu \propto M_5^3$  (see Eq. (3)), the 5-dimensional Planck mass is lowered, the inflaton mass ( $m$ ) becomes larger. This is in sharp contrast with a relation found in the RS brane-world cosmology [16],

$$\frac{m}{M_5} \simeq 1.26 \times 10^{-4} \left( \frac{60.5}{N_0 + 1/2} \right)^{5/6}, \quad (25)$$

where the inflaton mass becomes smaller as  $M_5$  is lowered.

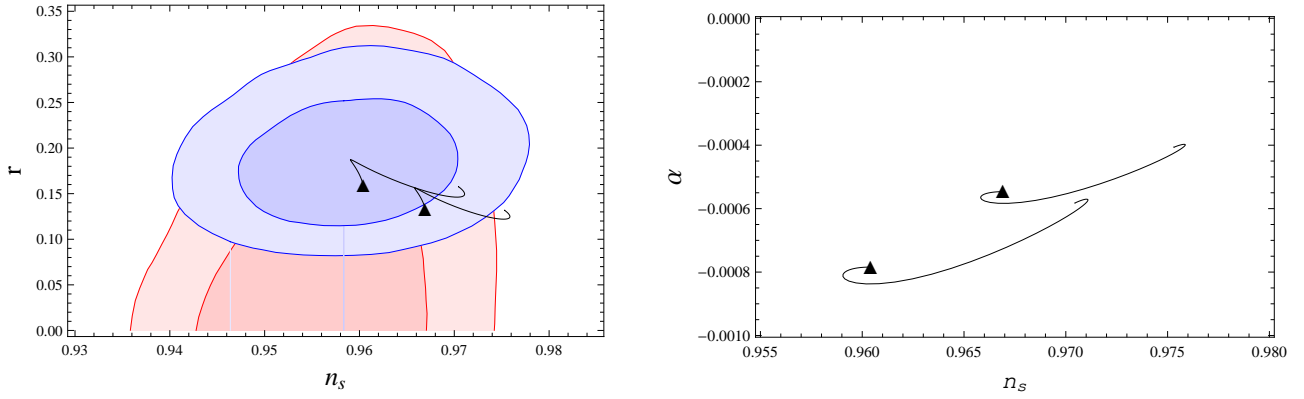


Figure 2: The inflationary predictions for the quadratic potential model:  $n_s$  vs.  $r$  (left panel) and  $n_s$  vs.  $\alpha$  (right panel) for various  $\mu$  values with  $N_0 = 50$  and 60 from left to right. The contours on the background are the 68% and the 95% C.L. from the Planck (Planck+WP+highL) [6] (shown in red) and the BICEP2 (Planck+WP+highL+BICEP2) [7] experiments (shown in blue). The black triangles are the predictions of the textbook quadratic potential model in the standard cosmology, which are reproduced for  $H/\mu \ll 1$ . As  $\mu$  is lowered, the inflationary predictions approach the values in Eq. (23). In each line, the turning points appear according to a non-trivial behavior of the first derivative of the Hubble parameter shown in the left panel of Fig. 1.

We calculate the inflationary predictions for various values of  $\mu$  with fixed e-folding numbers, and show the results in Fig. 2. In the left panel, the inflationary predictions for  $N_0 = 50$  and 60 from left to right are shown, along with the contours (at the confidence levels of 68% and 95%) from the Planck (Planck+WP+highL) [6] and the BICEP2 (Planck+WP+highL+BICEP2) [7]. The black triangles represent the predictions of the quadratic potential model in the standard cosmology. As  $\mu$  is lowered, the inflationary predictions approach the values in Eq. (23). In each line, the turning points appear according to a non-trivial behaviors of the first derivative of the Hubble parameter shown in the left panel of Fig. 1. For various values of  $\mu$ , the



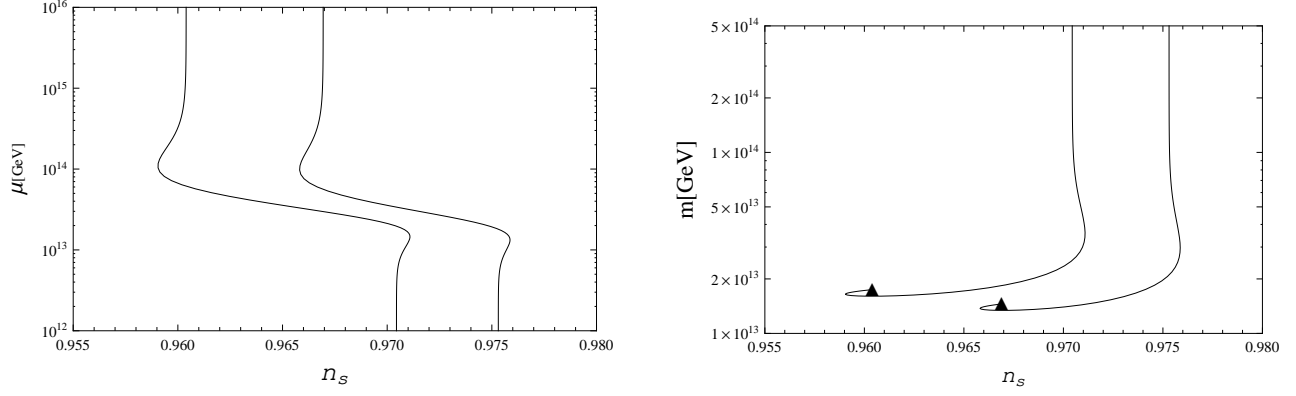


Figure 3: Relations between  $n_s$  and  $\mu$  (left panel) and between  $n_s$  and  $m$  (right panel), for  $N_0 = 50$  and 60 from left to right. The black triangles denote the predictions in the standard cosmology.

inflationary predictions are consistent with the BICEP2 result with  $r \gtrsim 0.1$ , which will be confirmed/excluded in the near future. The results for the running of the spectral index ( $n_s$  vs.  $\alpha$ ) is shown in the right panel, for  $N_0 = 50$  and 60 from left to right. We also show our results for the relations between  $n_s$  vs.  $\mu$ , and  $n_s$  vs.  $m$  in Fig. 3. Comparing two panels in Fig. 3, the inflaton mass is increased as  $\mu$  is lowered.

Next we analyze the textbook quartic potential model,

$$V = \frac{\lambda}{4!} \phi^4. \quad (26)$$

In the standard cosmology, we find the following inflationary predictions:

$$n_s = 1 - \frac{6}{2N_0 + 3}, \quad r = \frac{32}{2N_0 + 3}, \quad \alpha = -\frac{12}{(2N_0 + 3)^2}. \quad (27)$$

The quartic coupling ( $\lambda$ ) is determined by the power spectrum measured by the Planck satellite experiment,  $\mathcal{P}_S(k_0) = 2.215 \times 10^{-9}$  at the pivot scale  $k_0 = 0.05 \text{ Mpc}^{-1}$ , as

$$\lambda = 8.46 \times 10^{-13} \left( \frac{123}{2N_0 + 3} \right)^3. \quad (28)$$

We calculate the inflationary predictions for various values of  $\mu$  with fixed e-folding numbers  $N_0 = 50$  and 60. Our results are shown in Fig. 4. In the left panel, the inflationary predictions for  $N_0 = 50$  and 60 from left to right are shown, along with the contours (at the confidence levels of 68% and 95%) from the Planck and the BICEP2 experiments, as in Fig. 1. The results for the running of the spectral index ( $n_s$  vs.  $\alpha$ ) is shown in the right panel, for  $N_0 = 50$  and 60 from left to right. The black points represent the predictions in the standard cosmology presented



above. In Fig. 4, the inflationary predictions are moving anti-clockwise along the contours as  $\mu$  is lowered. The inflationary predictions for the standard cosmology are not preferable to the observation. For suitable values of  $\mu$ , the GB brane-world cosmological effect can slightly improve the fit of the BICEP2 result. We also show corresponding results for the relations between  $n_s$  vs.  $\mu$ , and  $n_s$  vs.  $\lambda$  in Fig. 5.

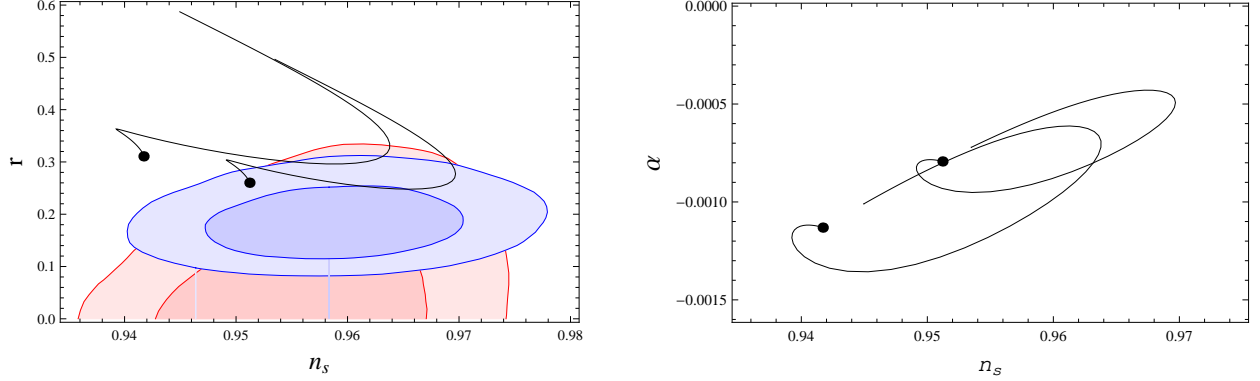


Figure 4: The inflationary predictions for the quartic potential model:  $n_s$  vs.  $r$  (left panel) and  $n_s$  vs.  $\alpha$  (right panel) with various  $\mu$  values for  $N_0 = 50$  and  $60$  from left to right. The contours on the background are the same as in Fig. 2. The black points are the predictions of the textbook quartic potential model in the standard cosmology. The inflationary predictions are moving anti-clockwise along the contours as  $\mu$  is lowered.

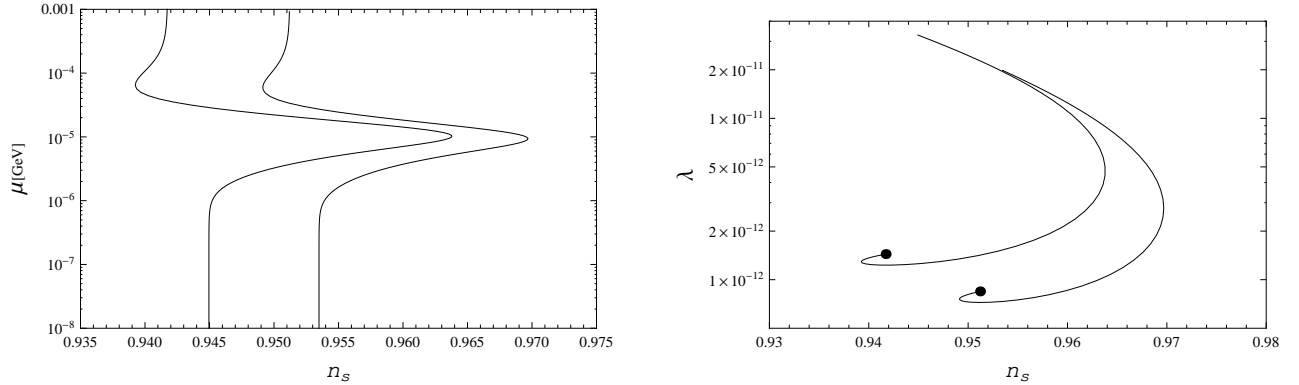


Figure 5: Relations between  $n_s$  and  $\mu$  (left panel) and between  $n_s$  and  $\lambda$  (right-panel), for  $N_0 = 50$  and  $60$  from left to right. The black points denote the values obtained in the standard cosmology.



### 3.2 Higgs potential model

The next simple inflationary model we will consider is based on the Higgs potential of the form [25]

$$V = \lambda (\phi^2 - v^2)^2, \quad (29)$$

where  $\lambda$  is a real, positive coupling constant,  $v$  is a VEV of the inflaton  $\phi$ . Here, we assume that the inflaton is a real scalar for simplicity, but it is easy to extend the present model to the Higgs model where the inflaton field breaks a gauge symmetry by its VEV. We refer, for example, Refs. [26, 27] for recent discussion about such a class of inflationary models, where quantum corrections of the Higgs potential are also taken into account.

For analysis of this inflationary scenario, we can, in general, consider two cases for the initial inflaton VEVs, namely, (i)  $\phi_0 > v$  and (ii)  $\phi_0 < v$ . However, in this paper, we concentrate on the case (ii), since the results for the case (i) are largely covered by those in the previous subsection. To see this, we rewrite the potential in terms of a new inflaton field  $\chi$  defined as  $\phi = \chi + v$ ,

$$V = \lambda (4v^2\chi^2 + 4v\chi^3 + \chi^4). \quad (30)$$

Clearly, an initial value of inflaton ( $\chi_0$ ) satisfies a condition,  $\chi_0/v \ll 1$ , the inflaton potential is dominated by the quadratic term. Hence, the inflationary predictions are similar to those for the textbook quadratic potential model. On the other hand, a condition of  $\chi_0/v \gg 1$  is satisfied, the quartic term dominates the inflaton potential, and the inflationary predictions in this case are covered by the analysis for the textbook quartic potential model. Therefore, the inflationary predictions of the model in the case (i) interpolate the inflationary predictions of the textbook quadratic and quartic potential models by varying the inflation VEV from  $v = 0$  to  $v \gg 1$ .

We now consider the GB brane-world cosmological effects on the Higgs potential model in the case (ii) and calculate the inflationary predictions for various values of  $\mu$  and  $v = 20, 30$  and  $100$ . Our results are shown in Fig. 6 for  $N_0 = 50$ . The black squares from bottom to top (top to bottom) in the left panel (the right panel) denotes the inflationary predictions in the standard cosmology limit for  $v = 20, 30$  and  $100$ , respectively. As  $v$  is raised, the predicted values of  $n_s$  and  $r$  in the standard cosmology approach those of the quadratic potential model (see the position marked by the black triangle in Fig. 2). As  $\mu$  is lowered, the inflationary predictions are deviating from the predictions in the standard cosmology. The inflationary predictions run away to the left as we lower  $\mu \lesssim 10^{13}$  GeV (see the left panel in Fig. 7), and hence we find a lower limit on  $\mu \gtrsim 10^{12}$  GeV to be consistent with the Planck measurement  $n_s \geq 0.936$ . We can



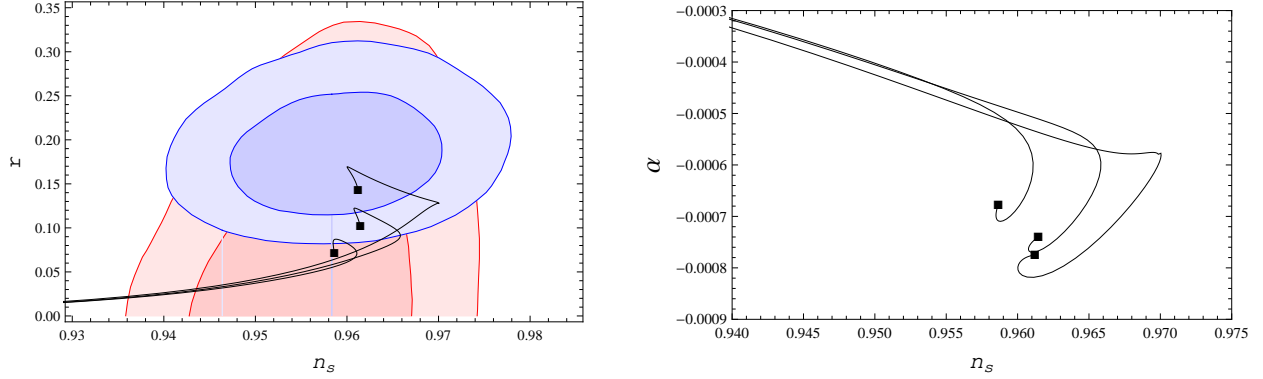


Figure 6: The inflationary predictions for the Higgs potential model:  $n_s$  vs.  $r$  (left panel) and  $n_s$  vs.  $\alpha$  (right panel) for various  $\mu$  values with fixed  $v = 20, 30$  and  $100$  from left to right. The contours on the background are the same as in Fig. 2. Here we have fixed the number of e-foldings  $N_0 = 50$ . The black squares from bottom to top (top to bottom) in the left panel (the right panel) denotes the inflationary predictions in the standard cosmology limit for  $v = 20, 30$  and  $100$ , respectively. As  $v$  is raised, the predicted values of  $n_s$  and  $r$  in the standard cosmology approach those of the quadratic potential model (see the position marked by the black triangle in Fig. 2). As  $\mu$  is lowered, the inflationary predictions are deviating from the predictions in the standard cosmology. When  $\mu$  is lower than  $10^{13}$  GeV (see the left panel in Fig. 7), the inflationary predictions run way to the left.

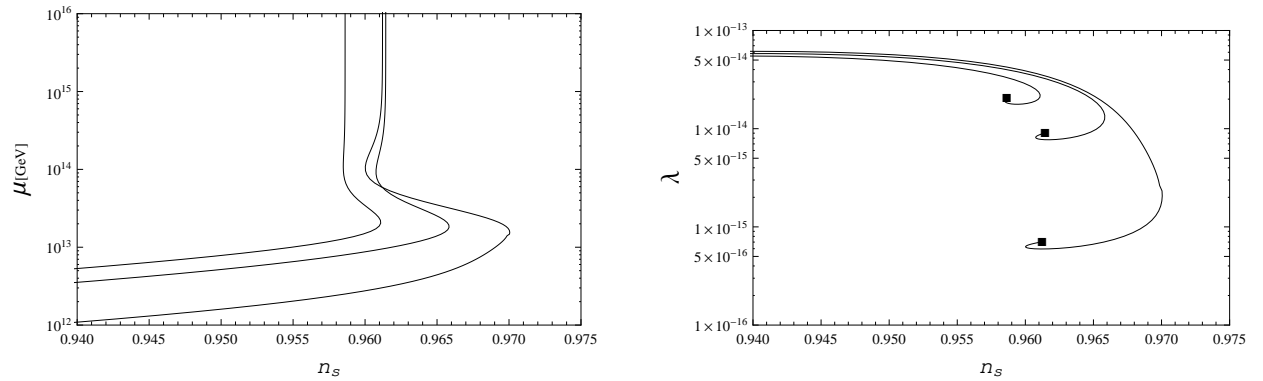


Figure 7: Relations between  $n_s$  and  $\mu$  (left panel) and between  $n_s$  and  $\lambda$  (right panel), corresponding to Fig. 6.



see that the brane-world cosmological effect suppresses the tensor-to-scalar ratio for  $\mu \lesssim 10^{14}$  GeV. Fig. 7 shows corresponding results in  $(n_s, \mu)$ -plane (left panel) and  $(n_s, \lambda)$ -plane (right panel). In the right panel, the black squares denote the results in the standard cosmology for  $v = 20, 30$  and  $100$  from top to bottom, respectively.

### 3.3 Coleman-Weinberg potential

Finally, we discuss an inflationary scenario based on a potential with a radiative symmetry breaking [28] via the Coleman-Weinberg mechanism [29]. We express the Coleman-Weinberg potential of the form,

$$V = \lambda \phi^4 \left[ \ln \left( \frac{\phi}{v} \right) - \frac{1}{4} \right] + \frac{\lambda v^4}{4}, \quad (31)$$

where  $\lambda$  is a dimensionless coupling constant, and  $v$  is the inflaton VEV. This potential has a minimum at  $\phi = v$  with a vanishing cosmological constant. Analysis for the Coleman-Weinberg potential model is quite analogous to the one of the Higgs potential model presented in the previous subsection. As same as the discussion about the Higgs potential model, we concentrate on the case  $\phi_0 < v$  for the initial VEV of the inflaton.

We show in Fig. 8 the inflationary predictions of the Coleman-Weinberg potential model for various values of  $v$  and  $\mu$  with  $N_0 = 50$ . The black squares from bottom to top (top to bottom) in the left panel (the right panel) denotes the inflationary predictions in the standard cosmology limit for  $v = 20, 30$  and  $100$ , respectively. As  $v$  is raised, the predicted values of  $n_s$  and  $r$  in the standard cosmology approach those of the quadratic potential model (see the position marked by the black triangle in Fig. 2). As in the Higgs potential model, lowering the  $\mu$  value deflects the inflationary predictions from those in the standard cosmology. The inflationary predictions run away to the left as we lower  $\mu \lesssim 10^{13}$  GeV, but they return to the right for  $\mu \lesssim 10^{10}$  GeV (see the left panel in Fig. 9). We find that the Planck measurement of  $n_s \geq 0.936$  excludes the range of  $10^9 \lesssim \mu [\text{GeV}] \lesssim 10^{12}$ . Fig. 9 shows corresponding results in  $(n_s, \mu)$ -plane (left panel) and  $(n_s, \lambda)$ -plane (right panel).

## 4 Conclusions

Today observational cosmology is a precision science, and the cosmological parameters are being very precisely measured. Motivated by the recent measurements of the CMB anisotropy by the WMAP and Planck satellite experiments and the observation of the CMB  $B$ -mode polarization announced by the BICEP2 collaboration, we have studied simple inflationary models based on



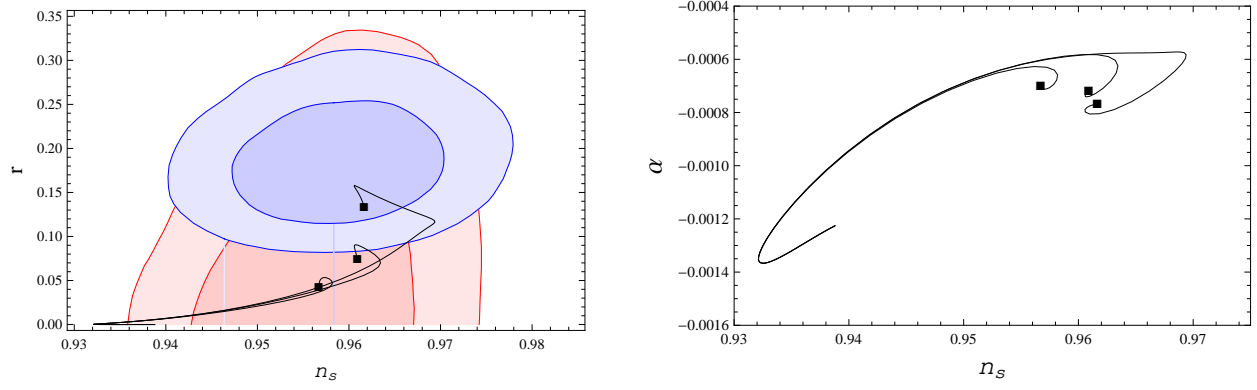


Figure 8: Same as Fig. 6 but for the Coleman-Weinberg potential model.

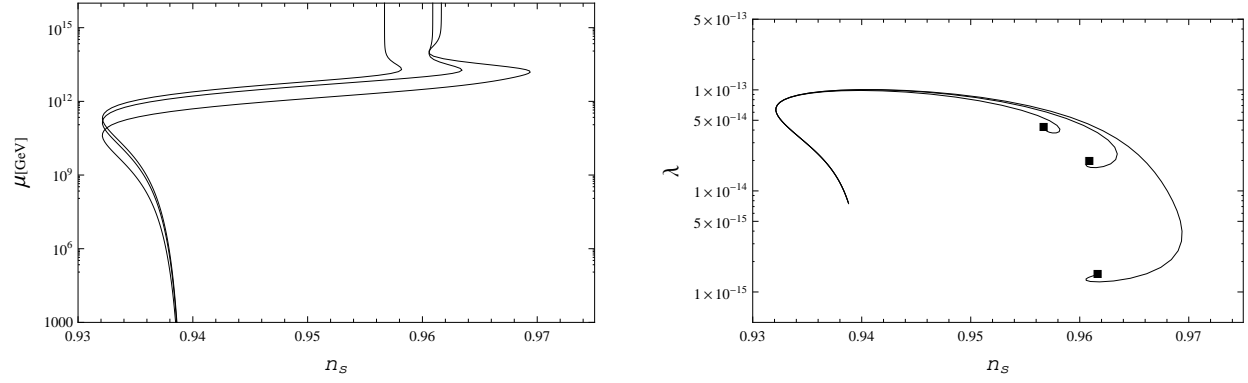


Figure 9: Same as Fig. 7 but for the Coleman-Weinberg potential model.



the quadratic, quartic, Higgs and Coleman-Weinberg potentials in the context of the Gauss-Bonnet brane-world cosmology. In the presence of the 5th dimensional space, not only the Friedmann equation for our 4-dimensional universe on the brane but also the evolution of scalar and tensor perturbations generated by inflation are modified and as a result, a drastic change of the inflationary predictions from those in the 4-dimensional standard cosmology can emerge. For the quadratic potential model, the GB brane-world cosmological effect makes the fit of the  $n_s$  prediction worse while the prediction for  $r$  is less modified. The GB brane-world effect can slightly improve the data fitting for the quartic potential model in a limited parameter region. The results for the Higgs and Coleman-Weinberg potential are similar and probably more interesting. When the GB brane-world cosmological effect is significant, the inflationary predictions of  $n_s$  and  $r$  are both suppressed and the current Planck measurement provides us with constraint on  $\mu$ , or equivalently, the 5-dimensional Planck mass. For the Higgs potential model with  $N_0 = 50$ , we have found an lower bound on  $\mu \gtrsim 10^{12}$  GeV (or, equivalently,  $M_5 \gtrsim 5 \times 10^{16}$  GeV) from the Planck measurement of  $n_s$ , while a range of  $10^9 \lesssim \mu[\text{GeV}] \lesssim 10^{12}$  (or, equivalently,  $5 \times 10^{15} \lesssim M_5[\text{GeV}] \gtrsim 5 \times 10^{16}$  GeV) is excluded for the Coleman-Weinberg potential model with  $N_0 = 50$ . It turns out that the GB brane-world cosmological effect causes a drastic change for the prediction of the spectral index, but a mild change for the tensor-to-scalar ratio. Therefore, a precise measurement of the spectral index in the future experiments can narrow an allowed region of the tensor-to-scalar ratio, which can be tested in the future observation of the CMB  $B$ -mode polarization.

In light of the recent observation of the  $B$ -mode polarization by the BICEP2 collaboration, simple inflationary models in the context of the Randall-Sundram brane-world cosmology have been investigated in [19]. It is interesting to compare the results presented in Sec. 3 in this manuscript to those presented in Sec. 2 in [19]. We can see that in the RS brane-world cosmology, the brane-world effect causes a drastic change (enhancement) for  $r$ , rather than  $n_s$ . This is in sharp contrast with the GB brane-world cosmological effect we have found in this paper.

## Acknowledgments

We would like to thank Andy Okada for his encouragements during the completion of the present work.

## References

- [1] A. A. Starobinsky, “A New Type of Isotropic Cosmological Models Without Singularity,” Phys. Lett. B **91**, 99 (1980).



- [2] A. H. Guth, “The Inflationary Universe: A Possible Solution to the Horizon and Flatness Problems,” *Phys. Rev. D* **23**, 347 (1981).
- [3] A. D. Linde, “Chaotic Inflation,” *Phys. Lett. B* **129**, 177 (1983).
- [4] A. Albrecht and P. J. Steinhardt, “Cosmology for Grand Unified Theories with Radiatively Induced Symmetry Breaking,” *Phys. Rev. Lett.* **48**, 1220 (1982).
- [5] G. Hinshaw *et al.* [WMAP Collaboration], “Nine-Year Wilkinson Microwave Anisotropy Probe (WMAP) Observations: Cosmological Parameter Results,” *Astrophys. J. Suppl.* **208**, 19 (2013) [arXiv:1212.5226 [astro-ph.CO]].
- [6] P. A. R. Ade *et al.* [Planck Collaboration], “Planck 2013 results. XVI. Cosmological parameters,” arXiv:1303.5076 [astro-ph.CO].
- [7] P. A. R. Ade *et al.* [BICEP2 Collaboration], “Detection of B-Mode Polarization at Degree Angular Scales by BICEP2,” *Phys. Rev. Lett.* **112**, 241101 (2014) [arXiv:1403.3985 [astro-ph.CO]].
- [8] B. Audren, D. G. Figueroa and T. Tram, “A note of clarification: BICEP2 and Planck are not in tension,” arXiv:1405.1390 [astro-ph.CO].
- [9] M. J. Mortonson and U. Seljak, “A joint analysis of Planck and BICEP2 B modes including dust polarization uncertainty,” arXiv:1405.5857 [astro-ph.CO]; R. Flauger, J. C. Hill and D. N. Spergel, “Toward an Understanding of Foreground Emission in the BICEP2 Region,” arXiv:1405.7351 [astro-ph.CO].
- [10] L. Randall and R. Sundrum, “An Alternative to compactification,” *Phys. Rev. Lett.* **83**, 4690 (1999) [hep-th/9906064].
- [11] P. Binetruy, C. Deffayet and D. Langlois, “Non-conventional cosmology from a brane-universe,” *Nucl. Phys. B* **565**, 269 (2000) [arXiv:hep-th/9905012]; P. Binetruy, C. Deffayet, U. Ellwanger and D. Langlois, “Brane cosmological evolution in a bulk with cosmological constant,” *Phys. Lett. B* **477**, 285 (2000) [arXiv:hep-th/9910219]; T. Shiromizu, K. i. Maeda and M. Sasaki, “The Einstein equations on the 3-brane world,” *Phys. Rev. D* **62**, 024012 (2000) [arXiv:gr-qc/9910076]; D. Ida, “Brane-world cosmology,” *JHEP* **0009**, 014 (2000) [arXiv:gr-qc/9912002].
- [12] For a review, see, e.g., D. Langlois, “Brane cosmology: An Introduction,” *Prog. Theor. Phys. Suppl.* **148**, 181 (2003) [hep-th/0209261].



- [13] N. Okada and O. Seto, “Relic density of dark matter in brane world cosmology,” *Phys. Rev. D* **70**, 083531 (2004) [arXiv:hep-ph/0407092]; T. Nihei, N. Okada and O. Seto, “Neutralino dark matter in brane world cosmology,” *Phys. Rev. D* **71**, 063535 (2005) [arXiv:hep-ph/0409219]; “Light wino dark matter in brane world cosmology,” *Phys. Rev. D* **73**, 063518 (2006) [arXiv:hep-ph/0509231]; E. Abou El Dahab and S. Khalil, “Cold dark matter in brane cosmology scenario,” *JHEP* **0609**, 042 (2006) [arXiv:hep-ph/0607180]; G. Panotopoulos, “Gravitino dark matter in brane-world cosmology,” *JCAP* **0705**, 016 (2007) [arXiv:hep-ph/0701233]; N. Okada and O. Seto, “Gravitino dark matter from increased thermal relic particles,” *Phys. Rev. D* **77**, 123505 (2008) [arXiv:0710.0449 [hep-ph]]; J. U. Kang and G. Panotopoulos, “Dark matter in supersymmetric models with axino LSP in Randall-Sundrum II brane model,” *JHEP* **0805**, 036 (2008) [arXiv:0805.0535 [hep-ph]]; W. -L. Guo and X. Zhang, “Constraints on Dark Matter Annihilation Cross Section in Scenarios of Brane-World and Quintessence,” *Phys. Rev. D* **79**, 115023 (2009) [arXiv:0904.2451 [hep-ph]]; S. Bailly, “Gravitino dark matter and the lithium primordial abundance within a pre-BBN modified expansion,” *JCAP* **1103**, 022 (2011) [arXiv:1008.2858 [hep-ph]]; M. T. Meehan and I. B. Whittingham, “Asymmetric dark matter in braneworld cosmology,” *JCAP* **1406**, 018 (2014) [arXiv:1403.6934 [astro-ph.CO]].
- [14] N. Okada and O. Seto, “Thermal leptogenesis in brane world cosmology,” *Phys. Rev. D* **73**, 063505 (2006) [arXiv:hep-ph/0507279]; M. C. Bento, R. Gonzalez Felipe and N. M. C. Santos, “Aspects of thermal leptogenesis in braneworld cosmology,” *Phys. Rev. D* **73**, 023506 (2006) [arXiv:hep-ph/0508213]; W. Abdallah, D. Delepine and S. Khalil, “TeV Scale Leptogenesis in B-L Model with Alternative Cosmologies,” *Phys. Lett. B* **725**, 361 (2013) [arXiv:1205.1503 [hep-ph]].
- [15] N. Okada and O. Seto, “A brane world cosmological solution to the gravitino problem,” *Phys. Rev. D* **71**, 023517 (2005) [arXiv:hep-ph/0407235]; E. J. Copeland and O. Seto, “Reheating and gravitino production in braneworld inflation,” *Phys. Rev. D* **72**, 023506 (2005) [arXiv:hep-ph/0505149]; N. M. C. Santos, “Gravitino production in the Randall-Sundrum II braneworld cosmology,” arXiv:hep-ph/0702200; W. Abdallah, D. Delepine and S. Khalil, “TeV Scale Leptogenesis in B-L Model with Alternative Cosmologies,” *Phys. Lett. B* **725**, 361 (2013) [arXiv:1205.1503 [hep-ph]].
- [16] R. Maartens, D. Wands, B. A. Bassett and I. Heard, “Chaotic inflation on the brane,” *Phys. Rev. D* **62**, 041301 (2000) [hep-ph/9912464].



- [17] D. Langlois, R. Maartens and D. Wands, “Gravitational waves from inflation on the brane,” *Phys. Lett. B* **489**, 259 (2000) [hep-th/0006007].
- [18] M. C. Bento, R. Gonzalez Felipe and N. M. C. Santos, “Brane-world inflation from an effective field theory after WMAP three-year data,” *Phys. Rev. D* **74**, 083503 (2006) [astro-ph/0606047].
- [19] N. Okada and S. Okada, “Simple brane-world inflationary models in light of BICEP2,” arXiv:1407.3544 [hep-ph].
- [20] J. E. Kim, B. Kyae and H. M. Lee, “Effective Gauss-Bonnet interaction in Randall-Sundrum compactification,” *Phys. Rev. D* **62**, 045013 (2000) [arXiv:hep-ph/9912344]; “Various modified solutions of the Randall-Sundrum model with the Gauss-Bonnet interaction,” *Nucl. Phys. B* **582**, 296 (2000) [Erratum-ibid. B **591**, 587 (2000)] [arXiv:hep-th/0004005]; S. Nojiri, S. D. Odintsov and S. Ogushi, “Friedmann-Robertson-Walker brane cosmological equations from the five-dimensional bulk (A)dS black hole,” *Int. J. Mod. Phys. A* **17**, 4809 (2002) [arXiv:hep-th/0205187]; J. E. Lidsey, S. Nojiri and S. D. Odintsov, “Brane-world cosmology in (anti)-de Sitter Einstein-Gauss-Bonnet-Maxwell gravity,” *JHEP* **0206**, 026 (2002) [arXiv:hep-th/0202198].
- [21] C. Charmousis and J. -F. Dufaux, “General Gauss-Bonnet brane cosmology,” *Class. Quant. Grav.* **19**, 4671 (2002) [hep-th/0202107]; K. -i. Maeda and T. Torii, “Covariant gravitational equations on brane world with Gauss-Bonnet term,” *Phys. Rev. D* **69**, 024002 (2004) [hep-th/0309152].
- [22] N. Okada and S. Okada, “Gauss-Bonnet brane-world cosmological effect on relic density of dark matter,” *Phys. Rev. D* **79**, 103528 (2009) [arXiv:0903.2384 [hep-ph]]; M. T. Meehan and I. B. Whittingham, “Dark matter relic density in Gauss-Bonnet brane-world cosmology,” arXiv:1404.4424 [astro-ph.CO].
- [23] J. F. Dufaux, J. E. Lidsey, R. Maartens and M. Sami, “Cosmological perturbations from brane inflation with a Gauss-Bonnet term,” *Phys. Rev. D* **70**, 083525 (2004) [hep-th/0404161].
- [24] J. E. Lidsey and N. J. Nunes, “Inflation in Gauss-Bonnet brane cosmology,” *Phys. Rev. D* **67**, 103510 (2003) [arXiv:astro-ph/0303168].
- [25] A. Vilenkin, “Topological inflation,” *Phys. Rev. Lett.* **72**, 3137 (1994) [hep-th/9402085]; A. D. Linde and D. A. Linde, “Topological defects as seeds for eternal inflation,” *Phys. Rev. D* **50**, 2456 (1994) [hep-th/9402115].



- [26] M. U. Rehman and Q. Shafi, “Higgs Inflation, Quantum Smearing and the Tensor to Scalar Ratio,” *Phys. Rev. D* **81**, 123525 (2010) [arXiv:1003.5915 [astro-ph.CO]].
- [27] N. Okada and Q. Shafi, “Observable Gravity Waves From  $U(1)_{B-L}$  Higgs and Coleman-Weinberg Inflation,” arXiv:1311.0921 [hep-ph].
- [28] Q. Shafi and A. Vilenkin, “Inflation with  $SU(5)$ ,” *Phys. Rev. Lett.* **52**, 691 (1984).
- [29] S. R. Coleman and E. J. Weinberg, “Radiative Corrections as the Origin of Spontaneous Symmetry Breaking,” *Phys. Rev. D* **7**, 1888 (1973).